Dielectric Probe of Intermolecular Interactions in Poly(methyl methacrylate) (PMMA) and PMMA + SiO 2 Matrixes Doped with Luminescent Organics

ARTICLE *in* THE JOURNAL OF PHYSICAL CHEMISTRY B · AUGUST 2001

Impact Factor: 3.3 · DOI: 10.1021/jp010618a

2 AUTHORS:

Ioannis M. Kalogeras
National and Kapodistrian University of Athens
40 PUBLICATIONS **605** CITATIONS
SEE PROFILE

Aglaia Vassilikou-Dova
National and Kapodistrian University of Athens
69 PUBLICATIONS **510** CITATIONS
SEE PROFILE

Dielectric Probe of Intermolecular Interactions in Poly(methyl methacrylate) (PMMA) and PMMA + SiO_2 Matrixes Doped with Luminescent Organics

Ioannis M. Kalogeras* and Aglaia Vassilikou-Dova

Section of Solid State Physics, Department of Physics, University of Athens, Panepistimiopolis, 157 84 Zografos, Hellas, Greece

Received: February 16, 2001; In Final Form: May 29, 2001

Modifications in the molecular dynamics of the side-chain relaxation in poly(methyl methacrylate) (PMMA) have been recorded by monitoring the thermally stimulated depolarization currents (TSDC) β-relaxation band of PMMA in three systems: bulk PMMA, PMMA polymerized in situ in porous SiO_2, and lasing matrixes with rhodamine 6G/Cl^- (R6G) and a perylene derivative (PG). To study the different types of inter- and intramolecular interactions, a range of dye concentrations and different polymerization initiators have been tested. In PMMA + SiO_2, the low-temperature (LT) shift of the β-band and the increase of the energy barriers (W) associated with the side-chain (re)orientation are attributed to various counterbalancing effects. A scheme of extensive hydrogen-bond interactions (*surface or chemical effect*) between the ester carbonyls of PMMA and the silicic acid pore surface is used to explain the overall increase in the distributed energy barriers. In contrast, the reduction of the polymer's chain entanglements and the increase in the free volume (*structural or physical effect*), due to the pore-directed polymerization, are considered to loosen up several steric hindrances on the rotational motion. The modification of the relaxation times spectrum prompts the shift of the β-relaxation in PMMA + SiO_2. In R6G + PMMA, the drastic LT shift of the β-band indicates the partial coupling between the chromophores and the side-group rotations. The TSDC spectrum does not present a rotational relaxation of the polar rhodamine dye. In R6G + PMMA + SiO_2, the presence of the chromophores on the pore surfaces and the corresponding decrease of the "effective" average pore diameters available for MMA diffusion and PMMA growth balance the physical and chemical effects, as depicted in the similarity of the energy distributions. The speedup of the β-relaxation with increasing dye content is ascribed to the reduced exposure of the side groups to chemical effects. The positive energy shift in PG + PMMA + SiO_2 can be explained by considering the mixing of PG and PMMA, which permits strong hydrogen-bonding interactions and simultaneously reduces PMMA's free volume. TSDC signals around room temperature (RT) are tentatively discussed in terms of a Maxwell−Wagner−Sillars (MWS) polarization mode at the PMMA−SiO_2 interface.

I. Introduction

During the past decades, particular attention has been given to the properties of low (usually glass-forming liquids) and high molecular weight materials confined in various porous media.[1] Nevertheless, relatively few reports are dedicated to dual matrixes prepared by impregnating micro- and mesopore media with polymers via the in situ polymerization of appropriate monomer−initiator solutions.[2−6] Inorganic−organic composites display a growing range of applications because of their improved optical, mechanical, thermal, and electrical characteristics. Poly(methyl methacrylate) (PMMA) is widely recognized as a polymer of high technological and industrial impact.[7] Owing to its excellent optical and mechanical properties, PMMA has been a first-choice component for the preparation of inorganic−organic composites.[8−10] Interesting examples of porous substrates are some natural and synthetic micropore structures (e.g., the zeolitic molecular sieves[2,11]) and especially the mesopore inorganic hosts (e.g., TiO_2 and SiO_2[2]) developed by the sol−gel method.[12] The controlled porosity (average pore diameters of about 5−20 nm) and homogeneity of the sol−gel processed materials allow their utilization as excellent thermally, chemically, and dimensionally stable matrixes (e.g., in pharmaceutical, medical, and optical applications) in virtually any form: monoliths, thin films, coatings, and composites.[12] The incorporation of the environmentally stable and optically transparent PMMA into the SiO_2 matrix (*index-matching* process) results in dual matrixes with a range of advanced physicochemical and mechanical characteristics[8,9] and multifunctional photonic applications.[13,14]

In this article, we present a dielectric study performed by means of the thermally stimulated depolarization currents (TSDC) technique[15] in a range of PMMA-based materials: bulk amorphous PMMA, diphasic PMMA + SiO_2 composites (PMMA polymerized in situ in 5 nm silica gels), and the same matrixes with dispersed laser-active dyes. The behavior of pure PMMA has been extensively studied, and several molecular relaxation mechanisms account for the explanation of dynamic mechanical and dc/ac dielectric signals (e.g., see references included in ref 6). In this study, confinement effects on the subglassy molecular relaxation processes of the macromolecules have been investigated, and the relative importance of the various types of interactions between the two chemically identifiable phases is being discussed. In the literature, controversial results appear on the effects of the restricted geometry on the molecular relaxation dynamics of the confined glass-forming liquids (form, strength, and frequency of relaxation of the intrinsic processes) and the molecular diffusion properties, compared to those of the bulk-liquid state. For glassy polymers embedded in porous matrixes, the scientific knowledge is far less developed. The geometrical restrictions influence the thermodynamic properties of the confined phase (either liquid or solid), e.g., by inducing new thermodynamic phases and by shifting characteristic phase transition temperatures,[6] as well as by changing the character of the transitions. The distinctive

* To whom correspondence should be addressed. E-mail: ikaloger@cc.uoa.gr.

10.1021/jp010618a CCC: $20.00
Published on Web 07/20/2001

mechanisms that can induce changes of the molecular dynamics can be categorized[1] as (a) *structural or "physical" effects* due to the variations of the steric hindrances in the limited volume, (b) *surface or "chemical" effects* owing to the wide range of molecular interactions at the phase boundaries, (c) *finite-size effects* due to the spatial heterogeneity of the confined material, and (d) *simple mixture effects* attributable to the topology, degree of order, and dimensionality of the confining phase. Their relative significance with respect to the materials presented in this study will be discussed in some detail.

For decades, the role of traps of photoactive, reactive, and bioactive molecules has been played primarily by inorganic and organic solutions, polymers, and ceramics. The sol−gel-derived pure SiO_2 and mixed glasses are a relatively new class of host matrixes. The chemistry and physics of the photonic applications employ a variety of photoprobes (e.g., fluorescent dyes and phosphorescent molecules) that show high selectivity and sensitivity to environmental parameters of the host, such as polarity, ionicity, viscosity, porosity, and local inclusion geometry.[16] In the field of laser applications, in particular, the nature of the host matrix has been shown to affect all characteristics of the dye. For instance, the host can (a) cause spectral shifts of the absorption and emission bands, (b) affect the photostability and the fluorescence quantum yield, (c) alter the relative importance of the processes by which the excited molecule relaxes (intersystem crossing, collisional energy loss, rotational and vibrational modes of energy dissipation, etc), and (d) consequently modify the fluorescence lifetime of the dye. Accordingly, the "compatibility" between the components in the lasing system is an essential parameter. In the above context, this paper attempts to relate, by using the TSDC method for the first time, aspects of the laser action of the dye molecules with specific interactions within the different solid-state environments provided for the preparation of solid-state dye laser materials. TSDC is a sensitive dc technique frequently used in performing a rapid characterization of materials through their dielectrically active relaxation phenomena. The technique is widely recognized as an efficient route for the determination of intra- and intermolecular interactions in polymer-based composites, mostly by monitoring their effects on the intrinsic dielectric relaxation mechanisms of the starting materials. The most common TSDC active mechanisms are[15] the orientational polarization of permanent molecular or ionic dipoles (e.g., the secondary relaxations of polar side groups in polymers), translational or space charge polarizations due to intrinsic free charges, interfacial polarizations in polycrystalline and multiphasic materials (e.g., the Maxwell−Wagner−Sillars, MWS, polarization mode), and relaxation effects from the homocharge injection from the electrodes (usually at high-poling fields).

The following study is part of a combined interdisciplinary investigation on the physicochemical and optical characterization of solid-state dye laser composites, involving studies of their lasing behavior and efficiency,[13,14] infrared and Raman spectroscopy studies,[3,5] differential scanning calorimetry (DSC)[4] studies, and dielectric relaxation[6,17−19] studies. A phenomenon with major industrial importance is the glass−rubber phase transition of polymers.[20,21] TSDC results in relation to the α-relaxation mechanisms in PMMA and PMMA + SiO_2 have been discussed in a previous paper.[6]

II. Experimental Section

II.A. Theory and Methods. The thermally stimulated depolarization current (TSDC) is a relatively simple technique widely used for the study of main and secondary dielectric relaxations in polymers.[15,20,21] A typical TSDC experiment consists of the polarization of the dielectric material at a sufficiently high temperature, T_p (polarization temperature), by applying an electric field, E_p (polarizing field), for a time, t_p (isothermal polarization time). In the next step, the temperature of the sample is lowered, with a controlled rate and with the electric field applied, to $T_0 \ll T_p$ at which the nonequilibrium state of the system is "frozen in". Finally, the sample is heated at a constant rate, b, while it is short-circuited through an ammeter, and the rate of depolarization (i.e., the current, $I(T)$) is recorded as a function of temperature. A TSD current peak is a result of two competing processes: (a) the increase of the relaxation frequency of the polarized entities with temperature which makes the current increase and (b) the gradual exhaustion of the polarization which induces a current decrease. The asymmetrical glow curve recorded during the TSDC experiment is described by

$$I_D(T) = \frac{P_0 S}{\tau_0} \exp\left[-\frac{W}{k_B T} - \frac{1}{b\tau_0} \int_{T_0}^{T} \exp\left(-\frac{W}{k_B T'} \right) dT' \right] \quad (1)$$

where P_0 is the saturation polarization of the specific relaxation mode, S is the sample's surface area, and k_B is the Boltzmann's constant. In accordance with the particular chemical, structural, and morphological characteristics of each material, the current peaks are assigned to orientational, space charge, or interfacial polarization relaxation phenomena. The study of a single current peak, i.e., a peak due to the uncorrelated relaxation of noninteracting dipoles, leads to the determination of the activation energy (W) and the preexponential factor (τ_0) using the Arrhenius equation for the relaxation time τ or, equivalently, the activation enthalpy (ΔH) and entropy (ΔS) using the Eyring formalism.[22] At temperatures below the glass−rubber transition temperature (T_g), the Arrhenius law is often used for the temperature-dependent relaxation time, $\tau(T)$,

$$\tau(T) = \tau_0 \exp\left(\frac{W}{kT}\right) \quad (2)$$

Equation 1 is deduced with this hypothesis and is similar to that describing thermoluminescence or thermostimulated conductivity processes obeying first-order kinetics.

Customarily, the results obtained from TSDC runs carried out in different experimental conditions and including a large number of experimental protocols, for example, the partial heating,[23] the peak cleaning,[15] and the thermal sampling (alternatively described as fractional or windowing polarization)[24] procedures, suggest that the current $I(T)$ is generally composed of several elementary components. Because most of the mechanical motions are excited in the TSDC spectrum, the interpretation of the molecular origin of several peaks in many polymers remains a controversial issue. Broad TSDC bands can be decomposed, at least theoretically, into an infinite number of elementary peaks. Consequently, broad distributions of simple exponential (Debye-type) processes due to the distribution of the relaxation parameters (τ_0, W) have to be considered.[15] For glassy polymers, this point of view is supported by the lack of order and the existence of different conformations of the macromolecules, together with the anisotropic degree of interactions between the relaxing units. The distribution becomes continuous when all dipoles, because varying dipole−dipole interactions and steric hindrance factors, have different relaxation times. In the case of an energy-distributed dipolar mechanism, as in the secondary relaxations of polar side groups in polymers, the thermocurrent signal can be expressed in the form

$$I_D(T) = \frac{P_0 S}{\tau_0}\int_0^\infty g_p(W)\exp\left[-\frac{W}{k_B T} - \frac{1}{b\tau_0}\int_{T_0}^{T}\exp\left(-\frac{W}{k_B T'}\right)dT'\right]dW \quad (3)$$

where $g_p(W)$ is the effective distribution function, representing the relative contributions of the elementary polarizations between W and $W + dW$ to the total dipolar relaxation strength.[15] The high resolution and the variability in the experimental procedures used in TSDC permit the study of the influence of the chromophores and the geometrical confinement in the dynamics of the subglassy molecular relaxation mechanisms of PMMA.

II.B. Experimental Detail. The 5-nm nominal pore diameter sol−gel SiO_2 glasses (densified at 1073 K) were provided by Geltech, Inc. (U.S.A.). The total pore volume of SiO_2 is 0.7 cm^3/gr, with a surface area of 580 m^2/gr. The bulk density of the unfilled SiO_2 is 0.9 gr/cm^3, and its specific density is 1.1 cm^3/gr. The mesoporous glass blocks are transparent with an ultraviolet (UV) cutoff at 0.3 μm and an infrared (IR) cutoff at 2.14 μm. Their composition is >99% silica (cation impurities, ~1 ppm). Prior to impregnation, the glass monoliths with typical dimensions of 5 mm × 5 mm × 10 mm were placed in a vacuum oven (1 Torr, 318 K) for 24 h.

The incorporation of the dyes in the PMMA and the composite PMMA + SiO_2 matrixes was performed following different procedures. The perylene green (PG, Figure 1a) dye is an uncharged compound with a relatively low melting point, relatively high vapor pressure, and good solubility in nonpolar solvents. Dissolving the dye in the liquid monomer (methyl methacrylate, MMA) was used to incorporate perylene into PMMA. The polymerization proceeded at 313 K for 3 days, initiated by 0.125% by mass of benzoyl peroxide dissolved into the MMA. The estimated dye concentration is 3×10^{-5} M for the PG + PMMA samples. Bulk PMMA samples were prepared with similar polymerization conditions. The incorporation of perylene green in the glass substrate was performed by dissolving the dye in the liquid monomer−initiator mixture, followed by polymerization within the porous skeleton. The estimated dye concentration for the PG + PMMA + SiO_2 samples is 10^{-4} M. PMMA + SiO_2 was prepared in a similar manner in the absence of the dye.

The highly ionic xanthine dye rhodamine 6G/Cl^- (R6G, Figure 1b) demonstrates good solubility in highly polar solvents such as alcohols but only slight solubility in the less polar MMA. Thus, dye impregnation was performed by mixing a 10^{-5} M dye solution in ethanol with MMA in a ratio of 8%:92% and polymerizing as above (dye concentration ~8×10^{-5} M). For the impregnation of the glass substrate with rhodamine, the following procedure has been used: the porous glass was immersed in an ethanolic solution of rhodamine for 2 weeks at a constant temperature of 313 K, followed by heat treatment in a vacuum in order to evaporate the solvent. Finally, the glass was immersed in the initiator−monomer solution, and the mixture was sealed in a test tube under air and heated to 313 K. The resulting R6G + PMMA + SiO_2 block has a dye concentration of ~12×10^{-5} M.

Neutron magnetic resonance and DSC studies suggest an amorphous macromolecular configuration with a high degree of syndiotactic character for both bulk PMMA and the polymer strands confined in the porous silica gel glass.[4] Fourier transform Raman (FT-Raman) studies indicate that the degree of MMA polymerization is lower in the glass (~10% nonpolymerized MMA), compared to bulk PMMA (~2−4% unconverted MMA).[5] The results from the nitrogen absorption and gel permeation chromatography studies show an increase of the average molecular weight (M_n, M_w) of PMMA in ~5 nm SiO_2 compared to bulk PMMA.[4]

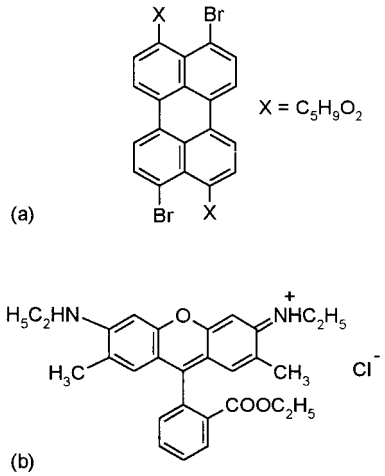

Figure 1. Molecular structures of the dyes perylene green (a) and rhodamine 6G/Cl^- (b).

The TSDC scans covered the range of 10−340 K and were performed in a vacuum of 10^{-3}−10^{-6} Torr. The apparatus used in the present study are described in detail elsewhere.[19] The typical TSDC experimental conditions of T_p = 320 K, E_p = (3−5) × 10^6 V/m, t_p = 5 min, T_0 = 10 K, and b = 5 K/min provided saturation polarization for the mechanisms activated below room temperature (RT). Prior to the measurements, all samples (of typical dimensions 5 mm × 5 mm × 1 mm) were stored under ambient conditions in protective packaging, which allowed them to absorb only small amounts of atmospheric H_2O vapors, in addition to the water inherited during the sample preparation procedures. Under extreme hydration conditions, the SiO_2 glass absorbs up to 30% of its dry weight. A measure of the relative affinity of each material in water absorption was given from the initial strength and the time evolution of the TSD current signals attributed to water.

III. Results and Discussion

III.A. PMMA and PMMA + SiO_2. The thermally stimulated depolarization current spectrum of conventionally polarized PMMA electrets is composed of three overlapping peaks in the range below room temperature.[6,11,15,17] Figure 2 presents the normalized TSDC spectra of bulk PMMA (plot a) and the composite PMMA + SiO_2 (plot b). The original thermograms were normalized to unit height for the dielectric β-relaxation maximum current I_m (i.e., plots of I/I_m vs absolute temperature). The main features in these spectra are the relatively weak band at ~70 K, associated with the rotation of the α-methyl in PMMA (γ-relaxation),[20] the current band in the region between 100 and 150 K, and the broad β-relaxation band (maxima: $T_\beta \approx$ 229 K in PMMA, 219 K in PMMA + SiO_2). The plots b−d shown in Figure 3 demonstrate the time evolution of the TSDC spectrum after keeping the polymer−glass block under high vacuum within the measuring cell at the constant aging temperature of 320 K.

The initially intense current band peaking at around 120−130 K is attributed to the reorientation of the water molecules trapped in the diphasic sample. According to FT-Raman and near-infrared (NIR) studies, the residual water inherited from the preparation process is not evenly distributed in the composite but locally enriched on the silica surface, hydrogen-bonded to limited surface silanols Si−OH.[3] After impregnation, the

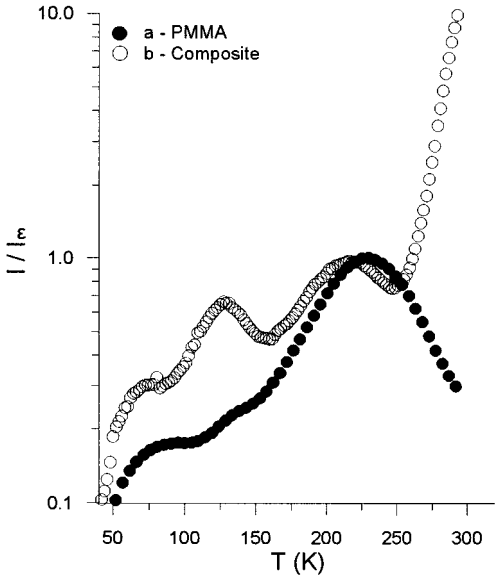

Figure 2. Normalized TSDC spectra of bulk PMMA (a) and the composite material PMMA + SiO_2 (b).

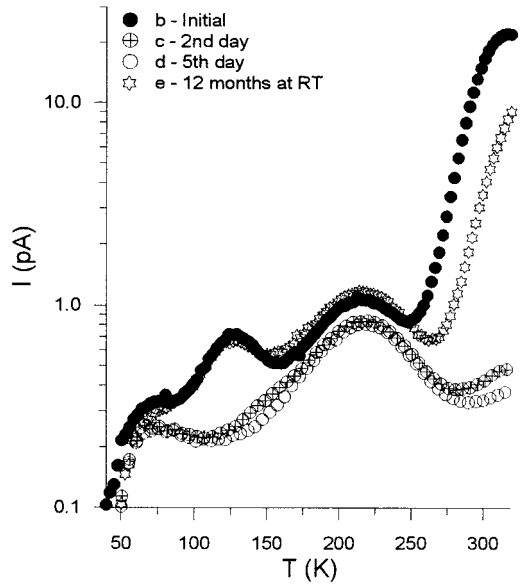

Figure 3. Time development of the TSDC spectrum of the PMMA + SiO_2 sample after keeping the sample under high vacuum at 320 K.

accessible water-adsorbing sites are highly reduced, while a small amount of the adsorbed water molecules is dispersed within the macromolecular component (as in pure PMMA[25]). The enhancement of the effective H_2O-trapping sites in the composite, due to the hydrophilic silanol groups at the pore surfaces and probably the increased free volume in the impregnated hydrophobic PMMA phase, explains the increased magnitude of the H_2O relaxation signal in the composite (Figure 2, plot b) compared to that in bulk PMMA (Figure 2, plot a). The slight high-temperature shift of the water peak with increasing aging time (Figure 3) can be explained by considering the entrapment of the polar H_2O molecules in different molecular environments. Following the established terminology, the water content can be categorized in bulk, loosely bound, and tightly bound fractions. These fractions relax at different temperature ranges of the TSDC spectrum.[26] Thus, the progressive high-temperature shift and weakening of the TSD current signal (Figure 3, plots b, c, and d) reflect the gradual desorption of water molecules. The loosely bonded fraction at the low-

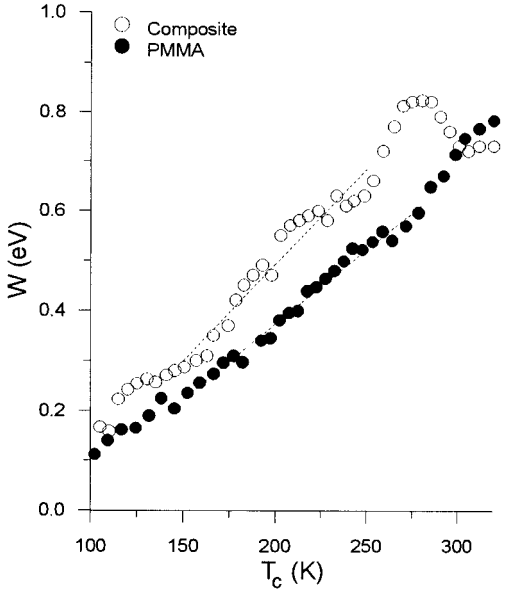

Figure 4. Plots of the activation energy barriers, *W*, as a function of the cutoff temperature, T_c, recorded for PMMA and PMMA + SiO_2 samples cut from the same block.

temperature side is the first to desorb because of the low pressure in the cell. By the end of the fifth day, the H_2O relaxation band only presents a weak bend in the rising part of the secondary β-relaxation of PMMA. Subsequent storage of the sample at ambient conditions for an extended period of time (~1 year) seems to restore the dielectric behavior of the composite to its initially recorded strength (Figure 3, plot e), indicating the reversibility of the desorption process.

The prominent dielectric effect in the TSDC spectrum of PMMA is the so-called secondary relaxation or β-relaxation, generated by the local motions of the carboxymethyl side groups of the macromolecular phase.[15,20,21,27] The ester carbonyl in the side group is the only strongly polar formation in this polymer. Thus, the dielectric strength of the β-relaxation band exceeds that of the primary relaxation band or α-relaxation band, related to the conformational main chain motions around T_g (observed at least 100 K above T_β[6,28]). The energy describing the rotation of the group around its bond with the main chain has a specific intramolecular barrier.[29,30] Additional contributions in the formation of the actual energy barrier arise from several local motions, e.g., rotations around the (O═)C−OCH_3 bond, rotations within the side group,[31] and torsion angles in the carbon chain. In addition, the α-methyl of PMMA impedes the rotation of the carboxymethyl side group.[21] For instance, the activation energy for the rotation of the α-methyl changes from 0.24 eV in isotactic PMMA to 0.33 eV in syndiotactic PMMA[32,33] because of the different degree of intermolecular interactions within the two stereoisomers.

According to Starkweather,[34,35] the secondary relaxation of PMMA is a noncooperative relaxation process and a distribution in the activation energies has to be invoked for the explanation of its non-Debye character in dielectric experiments. In the present case, for the decomposition of the broad TSDC spectra, we have employed the partial heating technique. Figure 4 demonstrates the variation of the activation energy barriers as a function of the cutoff temperature (T_c), for PMMA and PMMA + SiO_2, in the temperature range of the β-relaxation. The values have derived from the analysis of the partial discharge curves through the slope of the linear ln *I* vs 1/*T* plots (initial rise method[36]). The extensive energy distribution, observed between ~100 and 300 K in PMMA and ~150 and 250 K in the

composite, is associated with the intermolecular interactions that contribute to this relaxation, in addition to the intramolecular barrier.[30] At temperatures close to the low- and high-temperature sides of the β-relaxation peak in PMMA + SiO_2, the linearly increasing trend of the activation energies is disturbed because of the contributions from additional strong relaxation mechanisms. A direct comparison of the data in Figure 4 leads to the conclusion that the distribution of the energy barriers required for the activation of the dipole (re)orientation process is noticeably elevated in the composite. The energy difference around the β-peak maximum (at $T = T_\beta$), $\Delta W_\beta = W_\beta^{\text{confined}} - W_\beta^{\text{bulk}}$, is around +0.08 eV. The value of ΔW_β has to be considered cautiously because it is comparable to the estimated error of the initial rise method ($\leq \pm 8\%$, i.e., $\delta W \leq \pm 0.05$ eV for energies around 0.60 eV). Indeed, a drift of the β-relaxation energy distribution at higher values as a result of the confinement of PMMA in silica should normally lead to a high-temperature shift of the TSDC peak maximum. This has not been the case either in the present investigation (e.g., see Figure 2), where the free radical polymerization of the MMA monomers was initiated by benzoyl peroxide, or in our previous TSDC study of PMMA + SiO_2 composites prepared with variable contents of the initiator azo-bis-isobutyronitrile (ABIN).[6] In the study of ABIN, the β-relaxation peak has been found to shift to lower temperatures with increasing initiator content, e.g., from $T_\beta = 228$ K in PMMA prepared with 1 mg of ABIN/10 mL of MMA to ~221 K in PMMA with a 10-fold ABIN content. For PMMA + SiO_2 prepared with the above ABIN contents, T_β has been found to downshift by -17 ± 1 and -14.5 ± 1 K, respectively.[6,19] In the present case, the shift is around -10 K.

An attempt to explain this behavior will be presented in the following lines. According to the Bucci and Fieschi theory of TSDC,[37] there is an explicit relation of the peak maximum to the relaxation parameters of the dipoles population. Using the typical Arrhenius formalism, the maximum of a current peak, T_m, obeys the relation

$$\tau_0 = \frac{kT_m^{\,2}}{bW} \exp\left(\frac{-W}{kT_m}\right) \tag{4}$$

Given that the current contributions of the β-relaxation mechanism can be described by the Arrhenius equation and by considering as the set of characteristic relaxation parameters the values of the "effective" relaxation parameters (W', τ_0') associated with the population of dipoles disorientating around the peak T_β, the low-temperature shift is equivalent to a decrease of the characteristic preexponential factor, τ_0'. The relaxation time corresponds to the inverse of the frequency of jump between two activated states, while the preexponential factor relates to the inverse of the frequency of vibration at infinite temperature. The physical meaning of such a change in τ_0' becomes clearer within the Eyring's formalism in the theory of activated states in which the relaxation time is written as

$$\tau' = \frac{h}{kT} \exp\left(\frac{-\Delta S'}{k}\right) \exp\left(\frac{\Delta H'}{kT}\right) \tag{5}$$

h being the Planck's constant, with $\Delta H' = W' - kT$ and $\tau_0' \cong [h/(kT)] \exp(-\Delta S'/k)$. With the assumption of a constant activation enthalpy ($\Delta H' \approx W'$) for the dipolar β-relaxation mechanisms in PMMA and PMMA + SiO_2, the low-temperature shift can be explained as a result of an increase in the activation entropy. The increase should be more dramatic if we consider an energy increase, as determined with the partial heating technique (Figure 4). An increase in the activation entropy factor is a quite interesting variation if we bear in mind that for local, noncooperative relaxations, i.e., for relaxations involving the motion of small groups of atoms exhibiting *weak* interactions with other portions of the macromolecule or neighboring macromolecules, the (re)orientation process is considered to obey the zero entropy approximation, $\Delta S \approx 0$.[38,39] A tentative attribution of the change in ΔS can be put forward on the basis of the introduction of strong intermolecular interactions of the side chains with the inorganic substrate or a significant alteration of the typical rotation-hindering mechanisms found in bulk PMMA, due to its confinement in the porous environment. The low-temperature band's shift (i.e., faster relaxation) and the increase in the characteristic energy barrier (i.e., a slower response) may reflect the presence of several competing mechanisms controlling the molecular dynamics of PMMA. In the present case, the main contributions in the modification of the secondary relaxation are the following:

(a) PMMA is recognized as a basic polymer, or an electron donor, because of the electronegativity of the oxygen and the readily available lone pair electrons in the carbonyl group.[40] Such a basic polymer is susceptible to strong acid−base interactions with an acidic solvent (e.g., $CHCl_3$[41] and CH_2Cl_2[42]) or on acidic surfaces (e.g., inorganic fillers[43]). For example, in polymeric materials such as poly(methyl methacrylate), polyacrylate, polyimide, and polycarbonate interacting with silicon and fused silica surfaces, Spierings et al.[44] report high surfacial bond energies (~1 eV/nm^2 at RT). For silicates and precipitated silica gels, the concentration of the surface silanol (Si−OH) groups is drastically increased in comparison to fused silica because of the irreversible condensation of silanols to siloxanes (Si−O−Si). The very high surface area and surface free energy of the silica gel permit a strong interaction of basic PMMA with the silicic acid pore surface.[10] The hydrogen-bonding interaction scheme between the ester carbonyl groups of PMMA and surface silanols in mesoporous silica gel is widely accepted nowadays and has been adopted to explain experimental results from Mossbauer,[45] NIR,[3,46] FT-Raman,[3] DSC,[4] and dielectric relaxation spectroscopy (DRS)[6] studies. For example, the changes of the vibrational features of silanols on the silica surface and the ester carbonyls from PMMA are indicative of the hydrogen-bonding interaction (e.g., a shoulder at 1699 cm^{-1} on the 1725 cm^{-1} band assigned to the stretching mode of the C═O bond is attributed to the hydrogen-bonded side groups).[5] The extent of the polymer−SiO_2 hydrogen-bonding interaction is expected to induce an *increase* of the energy barrier required for (i) the rotation of a number of carboxymethyl side groups and (ii) the conformational motions of parts of the main chain in PMMA.[11]

(b) The silicon dioxide glasses are composed of a silica skeleton, which contains narrow channels. As a result of the pore-directed propagation of the MMA polymerization in SiO_2, the longitudinal PMMA chains fill most of these channels, in a degree related to the pore dimensions and polymerization conditions, to form a nonporous organic composite glass. The reduction of the chain entanglements due to the longitudinal arrangement of the PMMA macromolecules, with a concomitant increase of the free volume in the polymeric component, is expected to loosen several steric hindrances on the rotational motion of the side groups. In addition, besides its classification as a basic polymer, PMMA also possesses an amphoteric character due to the low acidity of the β-methyl at the side group. In bulk PMMA, interactions between chains can lead to self-associations toward the acrylate groups. Apparently, in the present case, this effect is suppressed because of the pore-

directed propagation of polymerization within the SiO_2 substrate. Thus, a *decrease* in the mean rotational energy barrier of the carboxymethyl groups is to be expected.

The interpretation of the data can thus be based on a two-stage model: a relatively immobile surface part with dynamics clearly determined by polymer−wall interactions and a volume part, which experiences the confinement effect. In the present 5-nm silica substrates, the hydrogen-bonding interaction (*surface* or *chemical effect*) appears to have increased relative weight in the formation of the overall energy barrier compared to the inner sterically eased PMMA phase (*structural* or *physical effect*). We should note that further studies, employing materials with a range of pore sizes, are required to quantify the relative importance of these mechanisms in connection with the openness of the pore structure. Systematic studies on this issue can be found in the literature *only* for the case of the α-relaxation mechanisms in confined liquids.[1] In these studies, the difference between the confining length (i.e., pore size) and the cooperativity length (characteristic length of the transition) is a critical factor. For instance, recent studies conducted by Moller et al. on PMMA strands confined into 0.6−3.5 nm inorganic hosts (e.g., microporous zeolites NaY, mordenite, and ZSM-5 and mesoporous MCM-41 and -48) do not record the characteristic glass−rubber transition effect.[2] On the contrary, PMMA confined in mesoporous silica gels with 5−20 nm average pore diameters exhibits distinct α-relaxation TSD current bands[47] and DSC exothermic peaks[4] characteristic of the glass−rubber transition. The PMMA−silica interaction has a significant effect on the dynamics of the glass−rubber transition mechanism of PMMA by shifting T_g to higher values.[4,6,48] Note that the *finite-size* and *simple mixture effects*, which are related with inclusion phenomena extended over many interatomic and intermolecular distances, are expected to have a noticeable influence only on the cooperative long-chain motions (i.e., the α-relaxation) and not on the local relaxation of the polar side groups of PMMA.

The γ-relaxation process, with the weak TSDC signal in the temperature range below ∼90 K, is less vulnerable to intermolecular and inorganic−organic surface interactions because of its small size (and thus its efficient shielding from the esterified side groups) and the low polarity of the α-methyl group. As a result, the position of the γ-relaxation band is not clearly affected.

Typically, a reduction of the pore-filling factor is anticipated because of the volume shrinkage (∼10%) occurring during polymerization. Additional experimental evidences are needed to confirm the hypothesis that some hydrogen-bond interactions at the early polymerization stages act as an inhibiting factor for the densification process with a simultaneous decrease of the polymer's density in the confined phase.

The absence, in the low-temperature range of the TSDC spectra, of bands attributed to relaxations characteristic of the silica gel matrix can be explained after viewing typical properties of the relaxation processes in SiO_2. Customarily, in nonirradiated glasses, three types of dielectric relaxation phenomena are expected, namely, ions' long-range migration or conduction mechanisms (type I; e.g., in mixed alkali halide glasses), short-range or "dipole" relaxations (type II), and several network or "lattice vibration" phenomena (type III).[49] Type I and II phenomena are absent in pure SiO_2. On the other hand, type III network phenomena due to the relaxation of movements of parts of the network are mainly expected in the region where the glass approaches its annealing temperature. The room-temperature dielectric constant of insulating *fused* SiO_2 at 1 kHz is $\epsilon' \cong 3.8$[50] and exhibits a slight decrease at 4 K ($\Delta\epsilon'/\epsilon' \cong 0.008$).[51] Dielectric losses in *fused* SiO_2 are only observed at very low temperatures: A DRS band recorded in isothermal measurements ($T = 27$ K) has been ascribed to the vibration of oxygen linkages at the nearly linear Si−O−Si bonds. An extremely weak band, recorded at temperatures less than 1.3 K, is related to the presence of hydroxyls.[52] In TSDC and mechanical spectroscopy studies of silica, network relaxations are expected far above 500 K. In addition, two TSDC processes of electric polarization, i.e., the disorientation of Si_{i3}^+/O_1^- dipoles (where Si_{i3}^+ is a positively charged silicon and O_1^- a negatively charged oxygen, each one with a dangling bond) have been reported at scanning temperatures above 400 K.[53] The dielectric response of sol−gel-derived SiO_2 porous glasses has been studied by several research groups[54−59] and is discussed in a review paper by Hench and West.[12] The relatively low-temperature processing of the sol−gel process, compared to the conventional glass preparation fusion routes, decreases the dielectric polarization modes that initiate from bond breaking and defect creation in fused silica. The prominent relaxation mechanism in pure silica arises from the rotational motions of the free −OH groups with a room-temperature gigahertz relaxation signal.[57,59] Extensive water adsorption causes an enrichment of the dielectric relaxation response of the sol−gel-derived SiO_2, with additional relaxation mechanisms in the gigahertz frequency region.[59] Such relaxations are manifested in the 100−150 K temperature range of the corresponding TSDC spectra. The above arguments justify the absence of relaxation modes from the silica matrix in the temperature range under investigation. Indeed, preliminary low-temperature TSDC scans in porous SiO_2 (in nitrogen gas atmosphere) only recorded a complex water dipole relaxation band (in the range of ∼90−150 K) and a current rise above ∼200 K (presumably a H^+ conduction mechanism).[19] The vacuum treatment of the sample reduces the intensity of the TSDC spectrum with the simultaneous appearance of a weak relaxation peaking around 210 K.

Another significant observation in the high-temperature region of the TSDC spectrum of PMMA + SiO_2 is the intense current rise above 250 K (Figures 2 and 3). Two main polarization schemes may be considered for the explanation of this non-fully-developed band: (a) a signal corresponding to the low-temperature part of the α-relaxation of PMMA, which maximizes in the temperature interval between ∼330 K (for stereoregular isotactic PMMA) and ∼400 K (at the highly syndiotactic stereoisomer)[28,47]; (b) part of a MWS relaxation peak, i.e., the thermal release during the depolarization step of charges accumulated during the electret-forming polarization step at the interfaces between regions of different conductivity under conditions of dc conductivity (the so-called "conductivity current relaxation").[60]

Parallel DSC[4] and TSDC[6] studies determine glass transition temperatures in the range of 390−405 K (i.e., an atactic PMMA phase with high syndiotacticity). When it is kept in mind that the location of the polar units at the side groups of PMMA usually leads to a stronger β-signal as compared to the atactic or syndiotactic α-relaxation signals around RT,[28] the first scheme is highly unlikely (compare the signals presented in Figure 2). Plasticizing effects[20] on the α-relaxation from the water molecules and the monomers trapped in the composite[5] are insufficient to explain the experimental behavior. On the other hand, a MWS interfacial polarization mode is highly probable because of the inhomogeneity of our system with the relatively conductive organic phase confined in the insulating silica matrix. Water adsorption increases the conductivity of the polymeric phase, as well as the conductivity difference

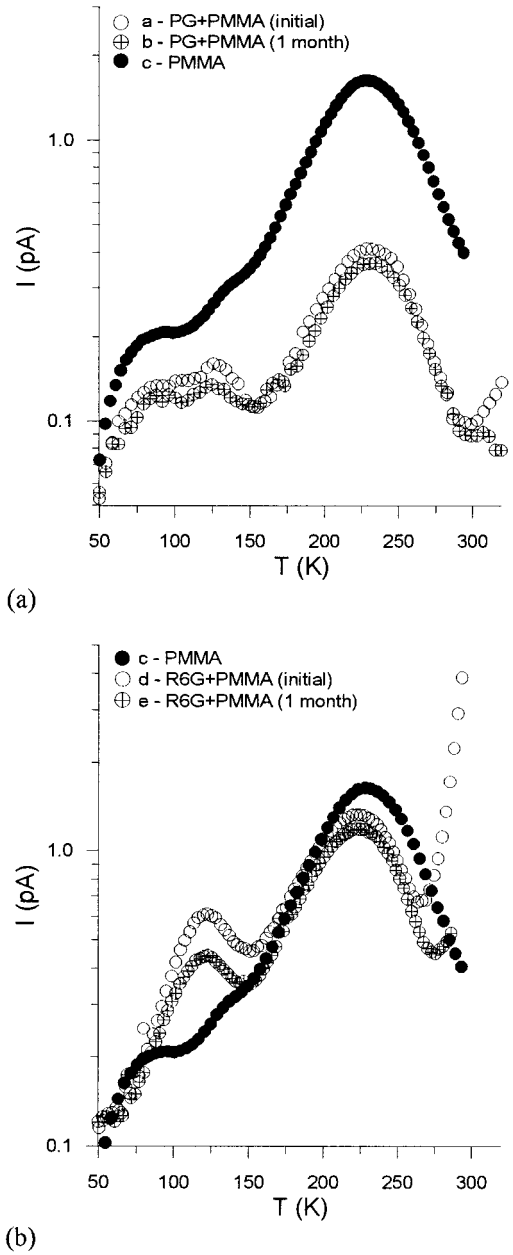

Figure 5. TSDC spectra of the PG + PMMA (a) and R6G + PMMA (b) blends. The development of the spectra after one month with the samples under high vacuum (at 320 K) is also presented.

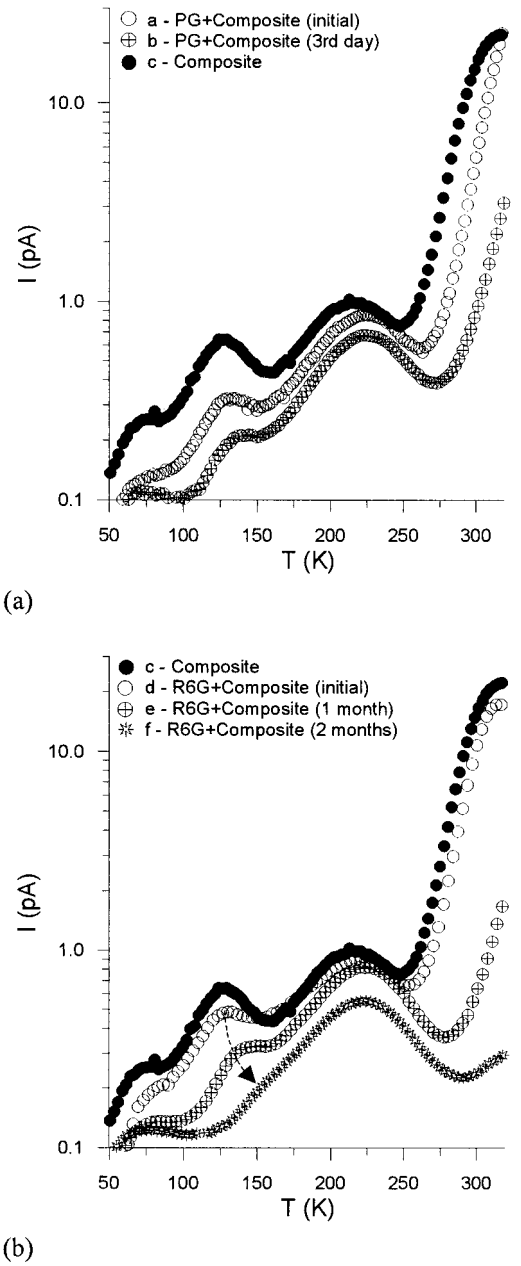

Figure 6. TSDC spectra of the dye composites PG + PMMA + SiO_2 (a) and R6G + PMMA + SiO_2 (b). The development of the spectra at selected times with the samples under high vacuum (at 320 K) is also presented.

between the two components, because of the introduction of mobile protons and charges produced by water-assisted dissociation processes in the macromolecules[61] and the pore surface. Note that a MWS interfacial relaxation mode is expected to reduce with the decrease of the conductivity in PMMA, i.e., by a decrease of the water content (represented by the area of the H_2O relaxation band in TSDC), in agreement with the results presented in Figure 3.

III.B. PMMA and PMMA + SiO_2 with R6G/Cl^- and PG. Figure 5 presents the current thermograms recorded for the blends of PG + PMMA (Figure 5a) and R6G + PMMA (Figure 5b). The TSDC spectrum of poly(methyl methacrylate) is included for comparison. The TSDC spectra of PMMA and PG + PMMA are identical. In the presence of the nonpolar perylene dye, no broadening or temperature shift of the β-relaxation band ($T_\beta = 231 \pm 1$ K) is observed. For the R6G + PMMA blend however, the secondary relaxation is downshifted to $T_\beta = 223 \pm 1$ K. In PG + PMMA, the weak relaxation band at $T_m = 130 \pm 2$ K decreases further after a few days of vacuum treatment. Similar behavior is also reported for PMMA blends with other perylene derivatives.[17] In the xanthine blend, the area of the band at 120 ± 1 K (representative of the mechanism's contribution in the static permittivity of the blend, $\Delta\epsilon$) and its temperature half-width ($\Delta T \approx 75$ K) exceeds those in bulk PMMA and PG + PMMA (e.g., $\Delta T \approx 50$ K). In addition, the band presents a greater resistance to evacuation: even after 4 weeks of consecutive experimental runs and high-vacuum treatment, its strength remains close to the initial one. At the same time, only the intense current rise, recorded at temperatures above 275 K, manifests a relatively drastic decrease (compare plots d and e in Figure 5b).

Figure 6 presents the TSDC spectra of PG + PMMA + SiO_2 (Figure 6a) and R6G + PMMA + SiO_2 (Figure 6b). The initial TSDC record for PMMA + SiO_2 is presented for comparison. Both dye composites present a β-relaxation peak located

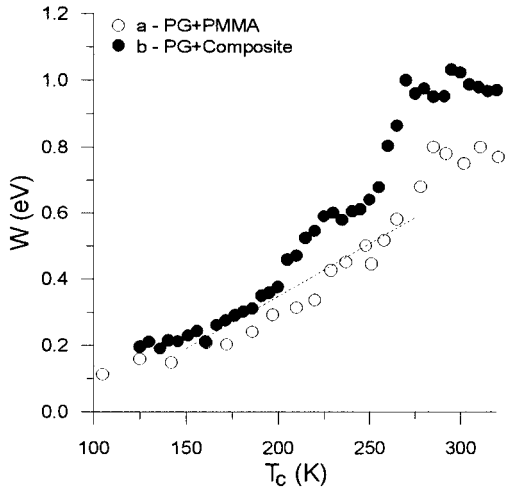

Figure 7. Plots of the activation energy barriers, W, as a function of the cutoff temperature, T_c, recorded for the blend PG + PMMA (a), the composite PG + PMMA + SiO_2 (b), and bulk PMMA (dashed line).

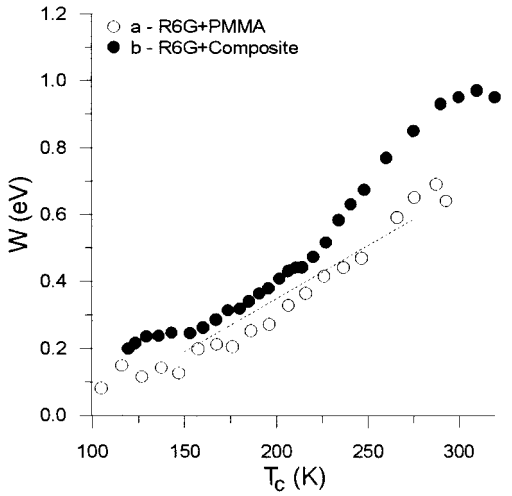

Figure 8. Plots of the activation energy barriers, W, as a function of the cutoff temperature, T_c, recorded for the blend R6G + PMMA (a), the composite R6G + PMMA + SiO_2 (b), and bulk PMMA (dashed line).

between the corresponding bands of bulk PMMA ($T_\beta = 229$ K) and PMMA + SiO_2 ($T_\beta = 219$ K). In the xanthine composite, the displacement of the β-relaxation signal is an increasing function of the R6G content, irrespective of the initiator type. For instance, in R6G + composites prepared using ABIN in the monomers solution, the β-relaxation band of bulk PMMA is located at $T_\beta = 240 \pm 1$ K and shifts at 220, 216, 215, and 212 K (± 2 K), by increasing the R6G content in the ethanolic dye solution to 10^{-5}, 5×10^{-5}, 10^{-4}, and 5×10^{-4} M, respectively. The position of the secondary relaxation band is nearly independent of the perylene dye content in PMMA or the PMMA + SiO_2 matrix, irrespective of the initiator used in the polymerization stage.[19] We should note that for the preparation of PMMA-based laser systems, azo-bis-isobutyronitrile is highly favored, compared to benzoyl peroxide, because chemical interactions between several dyes, like rhodamine 6G, and benzoyl peroxide have been found to modify the structure of the dye and deteriorate its laser action. Photodegradation mainly results from the existence of free radicals (and oxygen) in the polymer matrix. These radicals absorb the light during the operation of the laser and produce new radicals, and the interactions with R6G destroy the dye molecules permanently.[62] Weak chemical modifications of the molecular structures are connected with substantial shifts of the fluorescence wavelengths, in comparison to the unmodified dye molecules (i.e., the extreme case of the covalently bonded R6G and polymer matrix studied by Costela et al.[63]).

Figure 7 presents the variation of W vs T_c for the perylene blends with PMMA (plot a) and PMMA + SiO_2 (plot b) in the range of the secondary relaxation. Figure 8 presents the same dependence for the xanthine dye. The energy variation for bulk PMMA is given for comparison (dashed line). The partial discharge curves used for the energy estimations were recorded several days after the initial placement of the samples in the vacuum cell, ensuring the drastic reduction of the signals at the low- and high-temperature side of the β-relaxation signal. The purely organic materials (PMMA and dye + PMMA) exhibit nearly identical W vs T_c variation patterns.

The introduction of the chromophores brings to light a variety of new intermolecular interactions. In a recent report, Brower and Hayden[64] studied the effect of sub-T_g relaxations in the reorientation of several types of dye molecules in a series of corona-poled polymer hosts (PMMA, poly(ethyl methacrylate), and poly(isobutyl methacrylate)). Their experiments recorded a decrease in the activation volume for chromophore reorientation with increasing size of the polymer's alkyl side group. This effect has been considered to be a result of the partial coupling between chromophore rotation and the β-relaxation mode. In this TSDC study, the presence of intense coupling effects is manifested from the low-temperature shift of the β-relaxation band in the case of the R6G + PMMA blend. This mixture is the most interesting dielectric system because rhodamine 6G is regarded as a reference dye compound with laser characteristics frequently compared with the characteristics of novel molecules. In addition, the R6G + PMMA blend exhibits peculiar dielectric behavior. In a previous TSDC report of the R6G + PMMA mixture,[17] a much steeper energy variation has been recorded shortly after the placement of the sample in the cell. In that study, the difference, ΔW, in the values at the maximum, calculated before and after the vacuum and heat treatment, was near 0.2 eV. The temporal increase has been attributed to the hydrogen-bonding interaction between the small portion of the ethanol used as a solvent of the R6G molecules and the absorbed humidity with the carbonyl oxygen. The observation that ΔW is close to the energy of the hydrogen bond is in favor of this interpretation.[65]

The intense high-temperature signals in R6G + PMMA (Figure 6, plots a and b) can be related to a space charge relaxation mechanism involving protons and/or chloride anions. Given the relatively high energy of this relaxation ($\approx$1.2 eV around 300 K[17]), a Cl^- jump relaxation mechanism is the most likely contribution. The dye salt is fully dissociated in the polar ethanol environment,[16] as the high dielectric constant of the C_2H_5OH phase reduces to a great extent the strong electrostatic attraction between the pair components. Nonetheless, upon the removal of the polar solvent, the two components of the dye salt are expected to recombine. The concomitant decrease of the "effective" charge carriers normally reduces the magnitude of the electric conductivity signals. An alternative attribution would be a dipolar relaxation mechanism, i.e., the rotation of the Cl anion around the cationic dye ($R6G^+ - Cl^-$ dipole relaxation). The partial dissociation of the dye salt in the presence of the polar solvent environment increases the mobility for the chloride anions and reduces the energy barrier for local jumps around the bulky chromophore. After prolonged vacuum and thermal treatment and the gradual desorption of the polar

solvent molecules, the dye salt is expected to recombine. With the accompanying reduction in the Cl^- mobility (i.e., higher energy barrier), the band should normally decrease (as recorded in Figures 5b and 6b) or even shift to a higher temperature range outside our recording range. Similar reasoning may apply as well for explaining the behavior of the high-temperature signals in R6G + PMMA + SiO_2 (Figure 6b). For the composite, however, an intense conductivity band at the same temperature range is to be expected for reasons already discussed in the previous section (new defect sites with increased defect mobility, interfacial polarization modes, etc.). The role of new polarization modes in the composite material is clearly depicted in the difference observed between the high-temperature responses of PG + PMMA (Figure 5a, absence of relaxation signals in the range of 275−320 K) and those of PG + PMMA + SiO_2 (Figure 6a, intense signals around RT).

At temperatures above ~200 K, the β-relaxation energy spectrum exhibits a distinct elevation in the perylene composite and a much lower increase in the xanthine composite, compared to PMMA (see plots in Figures 7 and 8). These results can be connected to the different microenvironments of the side groups and the structural positioning of the organic oligomers. In R6G + PMMA + SiO_2, the chromophore molecules are attached to the pore surfaces by a number of weak (i.e., van der Waal's forces) and stronger interactions (hydrogen bonds with the silanols). As a result, the fluorescent molecules are evenly distributed in the internal porous surface of the inorganic component. The material can thus support a wider range of dye concentrations. Relatively high concentrations of R6G or other xanthine molecules are expected to increase the formation of fluorescent R6G J-dimers.[16,66] However, the rhodamine single molecules and the molecular complexes in R6G + PMMA + SiO_2 retain during polymerization their binding sites at the pore surfaces. This is supported by the absence of bleaching at the end of the polymerization.[13] As a result of the drastic decrease in parts of the channel openings available for MMA diffusion and PMMA growth, the surface and structural effects are well compensated. This explains the close proximity of the β-relaxation energy distribution patterns (Figure 8) in PMMA and R6G + PMMA + SiO_2. The increase of the low-temperature shift with increased shielding of the side groups by the dye molecules (at higher dye concentrations) is in favor of the above consideration. At the same time, a decrease in the openness of the pore network is expected to decrease the MMA-to-PMMA conversion rate. In PG + PMMA + SiO_2 on the other hand, the dye molecules and the macromolecular phase are ultimately mixed in the final polymerization product, allowing several hydrogen-bond susceptible sites in both the SiO_2 and PMMA phases. The highly effective surface−chemical interaction and the reduction of the polymer's free volume due to the presence of the bulky perylene molecules induce the behavior depicted in Figure 7.

A more precise examination of the TSDC spectra has been obtained by using the thermal sampling technique.[24] In the present study, we "sampled" the complex β-relaxation process by polarizing the specimens in the cooling stage within consecutive narrow temperature windows of $\Delta T = T_2 - T_1 = 5$ K ($-dT/dt = 5$ K/min, $t_p = 1$ min).[67] At the low-temperature side of each polarizing window (T_1), the sample remained short-circuited for 1 min. The nonequilibrium polarization state is maintained by cooling the sample to $T_0 \approx T_1 - 50$ K. In each of the subsequent heating stages, we recorded non-Debye current peaks. These peaks were further analyzed with a special fitting procedure[47] in order to obtain the main current contribution and its relaxation parameters (W, τ_0). A typical thermal sampling peak, recorded for the case of bulk PMMA, and the parameters of the corresponding fitting process are given in Figure 9. The relaxation parameters, which are of interest in each TS band, are those describing the main current contribution. Typically, the results of the TS technique are presented in the so-called relaxation maps, where one plots the activation energy (Figure 10) or τ_0 versus the central polarization temperature [$T_p = (T_2 - T_1)/2$]. In these plots, different cases can appear, e.g., (a) an indication of a distribution of the energy barriers with nearly constant τ_0 or (b) the variation of the preexponential factor with a stable activation energy (a rare situation). Figure 10 shows that W increases, but not linearly, with polarization temperature. In earlier TSDC studies of poly(methyl methacrylate),[68] W has been found to increase linearly with T with a slope of $dW/dT = 3.04 \times 10^{-3}$ eV/K. The data presented in Figure 10 can be best fitted with the logarithmic relations $\log W = -1.33 + 0.004T$ for PMMA and $\log W = -1.26 + 0.004T$ for R6G + PMMA + SiO_2. Note that the slopes are the same but different from that determined by Sauer and Avakian. The equality appears to corroborate their observation that the coefficient must

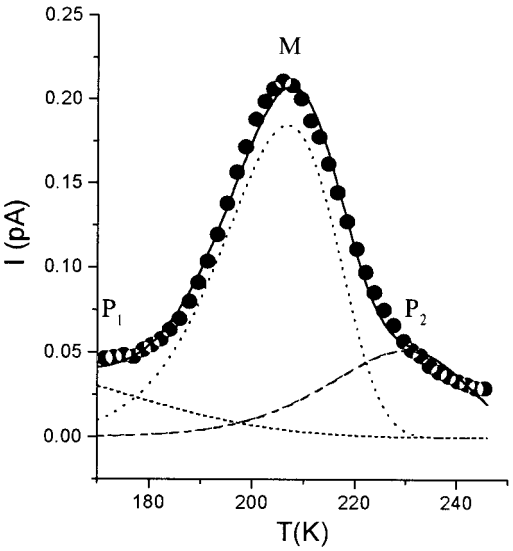

Figure 9. An example of the analysis of a complex TS peak (T_p = 190 K) into Debye-type (monoenergetic) components. The main band is characterized by $W = 0.32 \pm 0.01$ eV, $\tau_0 = 1.3 \times 10^{-6}$ s. The satellite peaks are characterized by energy barriers $W_1 = 0.03 \pm 0.01$ eV and $W_2 = 0.31 \pm 0.01$ eV.

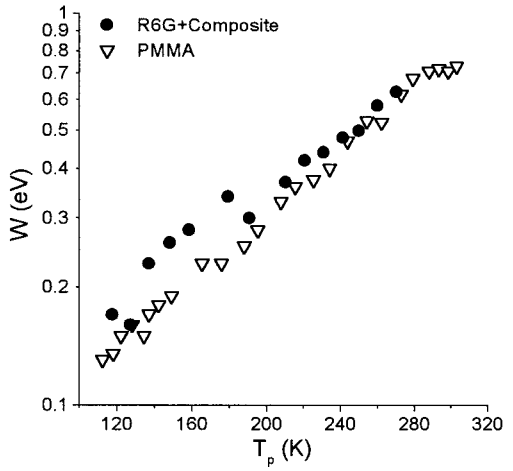

Figure 10. Plot of the activation energy versus the central polarization temperature of the TS peaks for bulk PMMA and R6G + PMMA + SiO_2.

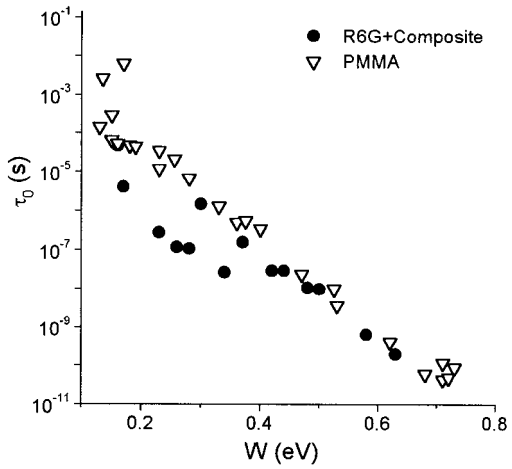

Figure 11. TS relaxation map showing the changes of W and τ_0 for bulk PMMA and R6G + PMMA + SiO_2.

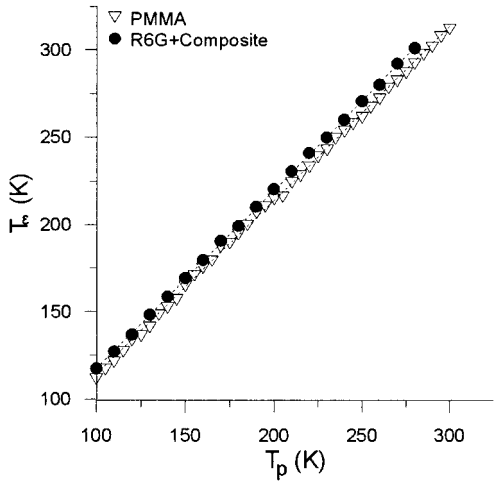

Figure 12. Plots of the characteristic temperature at current maximum, T_m, as a function of the polarization temperature, T_p, in each TS process for PMMA and R6G + PMMA + SiO_2.

be independent of the systems under study.[68] A third situation, frequently encountered in the TS relaxation maps, involves a strong linear correlation between the changes of W and τ_0. The last case is the so-called compensation law and is usually recorded for TSDC signals ascribed to the cooperative glass−rubber transition or other "cooperative" relaxations.[38,69] A fairly linear relation between the changes of W and τ_0 is depicted in Figure 11, which shows the plot of τ_0 vs W for bulk PMMA and R6G + PMMA + SiO_2. As expected, τ_0 decreases as W increases. For PMMA, the data can be fitted with the following equation: $\ln \tau_0 = -1.57 - 12.66W$. With the help of the relation

$$\ln \tau_0 = \ln \tau_c - \frac{W}{kT_c} \tag{6}$$

we calculate the following phenomenological compensation parameters: $\tau_c = 0.027 \pm 0.002$ s and $T_c = 394 \pm 11$ K. The points with $W < 0.20$ eV and $W > 0.65$ eV were excluded from the fitting procedure to use the most characteristic part of the spectrum (around T_β). For the R6G + PMMA + SiO_2 system, the data in the range of 0.30 eV $< W <$ 0.65 eV can be fitted with the equation $\ln \tau_0 = -2.5 - 11.41W$, which gives $\tau_c = 0.0031 \pm 0.0003$ s and $T_c = 437 \pm 12$ K.

The validity and the exact physical interpretation of the compensation law and the corresponding parameters are still under speculation.[38] For instance, the correlation between W and τ_0 is anticipated because the values of the activation energy and the inverse frequency factor (at infinite temperature) are interconnected by eq 4, which is valid for any TSDC peak. Thus, when the activation energy of a relaxation process increases, the preexponential factor will decrease necessarily in order to maintain the maximum of the peak in more or less the same temperature region. Irrespective of the existence of a true physical meaning for the compensation law, the errors for T_c are too significant to validate the existence of a compensation point for the β-relaxation,[38] either in bulk PMMA or in the polymer's environment provided by SiO_2 and the chromophores. This is to be expected from the noncooperative character of the local transition related to the secondary relaxation.

A strong indication for the absence of any hidden relaxation signal merged with the broad β-relaxation signal in R6G + PMMA + SiO_2 is given in Figure 12. In this plot, we present the variation of the characteristic temperature at the maximum of the current (T_m) as a function of the central polarization temperature (T_p) in each sampling procedure for PMMA and the composite. The linear dependences between T_m and T_p (slopes of 0.998 and 1.022 for PMMA and R6G + PMMA + SiO_2, respectively) are characteristic of a unique dipolar relaxation mechanism with a continuous distribution in the relaxation parameters.[24] The linearity extends even in the low-temperature side of the β-relaxation band as the H_2O relaxation signals are drastically reduced in the course of consecutive experimental runs. In R6G + PMMA + SiO_2, for polarization temperatures above 280 K, current rises dominate the TS spectra.

In Figure 13, we have plotted experimental parameters that appear to be representative of the fraction of the dipole population reorienting with a specific energy barrier. These are the maximum current, I_m (Figure 13a), and the TS peak's area, A (Figure 13b), plotted as a function of W. Peak's area is proportional to the image charge released from the electrodes during heating with rate b ($A = Qb$). These plots suggest some properties of the distribution function of the energy barriers. The distribution function for the secondary relaxation in pure PMMA appears symmetrical; the number of molecules experiencing a specific energy barrier increases smoothly with W up to a maximum value, which corresponds to the characteristic energy barrier W' at the maximum of the global β-relaxation peak, and then decreases in a similarly smooth way. In the composite, the asymmetric behavior recorded for $W \geq 0.6$ eV is related to the presence of intense current contributions for the high-temperature relaxation mechanism. Both graphs demonstrate nearly identical characteristic energy parameters for the secondary relaxation, with a difference ΔW_β in the energy values at the maximum of the peaks of around +0.02 eV, in agreement with the partial heating results in Figure 8.

The changes in the lasing properties of rhodamine 6G immersed in different carriers such as the organic solvents and solid-state hosts can be rationalized in terms of both the accompanying changes in the environmental polarity and a gradual change in the environment of the chromophores. In passing from the typical liquid solution media to adsorbates with increased matrix rigidity, a substantial hindering of the internal rotational relaxation modes of the dyes is anticipated.[13,70] The stabilization of the fluorescing component is an immediate consequence. In dielectric spectroscopy studies, the effects of, for example, the reduction of the effective "free-volume" or the direct covalent bonding to polymeric chains[71] on the molecular mobilities of the relaxing entities can be monitored. In the present study, the absence of any distinct TSDC relaxation peak due to the mobility of the polar and highly ionic

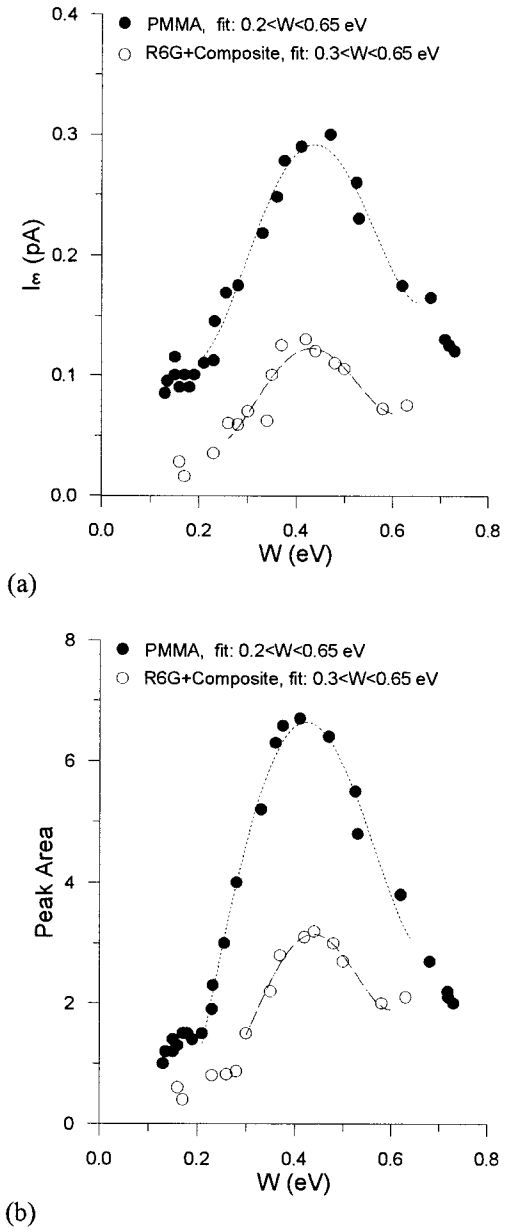

Figure 13. Plots of the maximum current, I_m (a), and the TS peak's area, A (b), as a function of the activation energy, W, for bulk PMMA and R6G + PMMA + SiO_2.

chromophores suggests that the immobilization of the R6G molecules quenches effectively the dielectrically active rotations of the polar carboxyethyl group, in the phenyl side group of rhodamine 6G.

Recent studies[13] demonstrate that the "sol−gel-philic" R6G dye shows better photostability and better radiation efficiency in the purely SiO_2 sol−gel-derived glass, compared to PMMA or even PMMA + SiO_2, because the SiO_2 rigid cage quenches, to a greater degree, the reorientation mechanism of the chromophore. The high rigidity of the SiO_2 matrix can be contrasted with the loose arrangement of the polymeric phase. The remaining mobility of the macromolecular chains in relatively loosely packed (low-density) regions within PMMA is considered to be responsible for intense structural relaxation phenomena[18,72] recorded at temperatures far below its glass−rubber transition temperature. Increased laser damage thresholds have been recorded for poly(methyl methacrylate) modified by the addition of ethanol,[73,74] probably for reasons related to the strong interactions of the dye with the polar alcoholic phase. We should note that the "sol−gel-phobic" perylene derivatives perform better in the organic PMMA and the composite PMMA + SiO_2 hosts,[75] compared to the pure SiO_2 or ormosil hosts. Given the fact that in the composite, the immediate environment of the dye molecules is PMMA, the relative gains of using PMMA + SiO_2 over PMMA have to be related to special characteristics of the inorganic component (i.e., its high thermal conductivity that reduces thermal lensing effects and the improved transparency in the UV and IR regions over PMMA). The silica skeleton and the hydrogen bonds in the silica−PMMA interfaces are also expected to influence the fluorescence characteristics.[76]

IV. Conclusions

Changes in the side-chain molecular dynamics of poly(methyl methacrylate) have been recorded by monitoring the behavior of the dielectric β-relaxation TSDC band of the polymeric phase in pure PMMA, within porous silica, and in lasing matrixes. In PMMA + SiO_2, the low-temperature shift of the β-peak with the simultaneous increase of the energy barrier associated with the corresponding molecular (re)orientation mechanism is attributed to the presence of various counterbalancing physical and chemical effects. A scheme of extensive hydrogen-bond interactions (surface or chemical effect) between the ester carbonyls of PMMA and the silicic acid pore surface is used to explain the overall increase in the energy barrier for dipole (re)-orientation. In contrast, the reduction of the polymer's chain entanglements and the increase in the free volume (structural or physical effect), due to the pore-directed polymerization process, are expected to loosen several steric hindrances on the rotational motion of the side groups. The corresponding modification in the spectrum of the relaxation times[77,78] induces the low-temperature shift of the dielectric β-relaxation band. TSDC signals from relaxation mechanisms intrinsic to the silica substrate are highly unlikely at the investigated temperature range, and thus, the peak's shift can be strictly related to phenomena arising from the geometrical confinement of the PMMA phase. The dielectric strength of the signals at the high-temperature part of the spectrum is highly dependent on the water content of the sample and accordingly the conductivity level of the polymeric phase. Hence, we tentatively relate these signals to a MWS polarization mode activating at the PMMA−SiO_2 interface.

A study of the porous silica sol−gel glasses impregnated with PMMA and lasing molecules is justified by their extensive implementation as hosts of different organic dyes in the research of advanced solid-state dye lasers. The incorporation of rhodamine 6G/Cl^- and perylene green in PMMA and composite PMMA + SiO_2 matrixes affects, to different degrees, the local β-relaxation mechanism of the polymeric component. The addition of the nonpolar perylene derivative in PMMA does not seem to change the relaxation parameters of the β-relaxation process. The situation changes dramatically with the introduction of the polar and highly ionic compound rhodamine 6G/Cl^-. In the R6G + PMMA blend, the drastic low-temperature shift of the secondary relaxation band indicates the partial coupling between the chromophore rotation and the rotation of the side groups in PMMA.[77]

The different balancing of the structural and surface effects becomes clearer by the direct comparison of the peak and energy shifts in PMMA + SiO_2 ($\Delta W_\beta = +0.08$ eV, $\Delta T_\beta = -10 \pm 1$ K) and the dye + PMMA + SiO_2 materials ($\Delta W_\beta = +0.02$ eV for R6G and +0.05 eV for PG, $\Delta T_\beta = -4 \pm 1$ K) with the values in bulk PMMA ($W_\beta = 0.42$ eV; $T_\beta = 229$ K). In R6G + PMMA + SiO_2, the presence of the dye molecules on the pore

surface and the corresponding decrease of the "effective" average pore diameter available for MMA diffusion and PMMA growth (i.e., reduced MMA-to-PMMA conversion) shift the balance between the surface and structural effects on the side of the second effect. The similarity between the distribution of the energy barriers in PMMA and that in R6G + PMMA + SiO_2 is in accordance with the above conclusion. The increase of the low-temperature shift of the TSDC band (i.e., a faster β-relaxation) with increasing dye concentration is attributed to the improved shielding of the side groups from hydrogen-bonding interactions due to the increased coverage of the pore surface by dye molecules. The positive energy shift in PG + PMMA + SiO_2 can be explained by considering that the dye molecules and the macromolecular phase are ultimately mixed in the final polymerization product. This allows the formation of several hydrogen bonds between silanols and the side groups of PMMA and at the same time a reduction of the polymer's free volume due to the bulky perylene molecules.

Acknowledgment. Financial support from the Solid Earth Physics Institute, Athens University is gratefully acknowledged.

References and Notes

(1) Pelster, R. *Phys. Rev. B* **1999**, *59*, 9214. Barut, G.; Pissis, P.; Pelster, R.; Nimtz, G. *Phys. Rev. Lett.* **1998**, *80*, 3543.
(2) Moller, K.; Bein, T.; Fischer, R. X. *Chem. Mater.* **1998**, *10*, 1841.
(3) Li, X. C.; King, T. A. *J. Sol−Gel Sci. Technol.* **1995**, *4*, 75.
(4) Pallikari-Viras, F.; Li, X. C.; King, T. A. *J. Sol−Gel Sci. Technol.* **1996**, *7*, 203.
(5) Li, X. C.; King, T. A.; Pallikari-Viras, F. *J. Non-Cryst. Solids* **1994**, *170*, 243. Pallikari, F.; Chondrokoukis, G.; Rebelakis, M.; Kotsalas, Y. *Mater. Res. Innovations* **2001**, *4*, 89.
(6) Kalogeras, I. M.; Vassilikou-Dova, A.; Neagu, E. R. *Mater. Res. Innovations* **2001**, *4*, 322.
(7) Billmeyer, F. W., Jr. *Textbook of Polymer Science*; Wiley & Sons: Singapore, 1984.
(8) Pope, E. J. A.; Asami, M.; Mackenzie, J. D. *J. Mater. Res.* **1989**, *4*, 1018.
(9) Abramoff, B.; Klein, L. C. *SPIE Sol−Gel Opt.* **1990**, *1328*, 241.
(10) Nobrega, M. C.; Gomes, L. C. F.; LaTorre, G. P.; West, J. K. *Mater. Charact.* **1998**, *40*, 1.
(11) Kalogeras, I. M.; Vassilikou-Dova, A. *Defect Diffus. Forum* **1998**, *164*, 1.
(12) Hench, L. L.; West, J. K. *Chem. Rev.* **1990**, *90*, 33.
(13) Rahn, M. D.; King, T. A. *Appl. Opt.* **1995**, *34*, 8260.
(14) Rahn, M. D.; King, T. A.; Gorman, A. A.; Hamblett, I. *Appl. Opt.* **1997**, *36*, 5862.
(15) Vanderschueren, J.; Gasiot, J. In *Field-Induced Thermally Stimulated Currents*; Sessler, G. M., Ed.; Topics in Applied Physics; Springer: Berlin, 1980.
(16) *Dye Lasers*; Schafer, F. P., Ed.; Topics in Applied Physics, Vol. 1; Springer: Berlin, 1990.
(17) Kalogeras, I. M.; Vassilikou-Dova, A. *Macromol. Symp.* **1999**, *148*, 301.
(18) Kalogeras, I. M.; Vassilikou-Dova, A. *Macromol. Symp.* **1999**, *148*, 285.
(19) Kalogeras, I. M. Ph.D. Thesis, University of Athens, 2000.
(20) Hedvig, P. *Dielectric Spectroscopy of Polymers*; Adam Hilger: Bristol, U.K. 1977.
(21) McCrum, N. G.; Read, B. E.; Williams, G. *Anelastic and Dielectric Effects in Polymeric Solids*; John Wiley: London, 1967.
(22) Starkweather, H. W. *Polymer* **1991**, *32*, 2443.
(23) Creswell, R. A.; Perlman, M. M. *J. Appl. Phys.* **1970**, *41*, 2365.
(24) Zielinski, M.; Kryszewski, M. *J. Electrost.* **1977**, *3*, 69.
(25) Drotning, W. D.; Roth, E. P. *J. Mater. Sci.* **1989**, *24*, 3137.
(26) Laudat, J.; Laudat, F. *Z. Phys. Chem.* **1991**, *174*, 211.
(27) Heijboer, J.; Baas, J. M. A.; Van der Graaf, B.; Hoefnagel, M. A. L. *Polymer* **1987**, *28*, 509.
(28) Gourari, A.; Bendaoud, M.; Lacabanne, C.; Boyer, R. F. *J. Polym. Sci. Phys.* **1985**, *23*, 889.
(29) Ishida, Y.; Yamafuji, K. *Kolloid−Z.* **1961**, *177*, 97.
(30) Shindo, H. *J. Sci. Hiroshima Univ., Ser. A−2* **1969**, *33*, 189.
(31) Gomez Ribelles, J. L.; Meseguer Duenas, J. M.; Monleon Pradas, M. *J. Appl. Polym. Sci.* **1989**, *38*, 1145.
(32) Allen, G.; Wright, C. J.; Higgins, J. S. *Polymer* **1974**, *15*, 319.
(33) Gabrys, B.; Higgins, J. S.; Ma, K. T.; Roots, J. E. *Macromolecules* **1984**, *17*, 560.
(34) Starkweather, H. W. *Macromolecules* **1988**, *21*, 1798.
(35) Starkweather, H. W. *Macromolecules* **1990**, *23*, 328.
(36) Garlick, G. F. J.; Gibson, A. F. *Proc. Phys. Soc., London, Sect. A* **1948**, *60*, 574.
(37) Bucci, C.; Fieschi, R.; Guidi, G. *Phys. Rev.* **1966**, *148*, 816.
(38) Sauer, B. B.; Moura Ramos, J. J. *Polymer* **1997**, *38*, 4065.
(39) Correia, N. T.; Alvarez, C.; Moura Ramos, J. J.; Descamps, M. *Chem. Phys.* **2000**, *252*, 151.
(40) (a) Fowkes, F. M. *J. Adhes. Sci. Technol.* **1987**, *1*, 7. (b) Fowkes, F. M.; Tischler, D. O.; Lannigan, J. A.; Ademu-John, C. M.; Halliwell, M. J. *J. Polym. Sci. Chem.* **1984**, *22*, 547.
(41) Bistac, S.; Schultz, J. *Prog. Org. Coat.* **1997**, *31*, 347.
(42) Hanumantha Rao, K.; Forssberg, K. S. E.; Forsling, W. *Colloids Surf. A* **1998**, *133*, 107.
(43) Fowkes, F. M. *Surface and Interface Aspects of Biomedical Polymers*; Andrade J. D., Ed.; Plenum: New York, 1985; Vol. 1, p 337. Iler, R. K. *The Chemistry of Silica: Solubility, Polymerization, Colloid and Surface Properties and Biochemistry*; Wiley-Interscience: New York, 1979.
(44) Spierings, G. A. C. M.; Haisma, J.; Vanderkruis, F. J. H. M. *Philips J. Res.* **1995**, *49*, 139.
(45) Leidheiser, H., Jr.; Deck, P. D. *Science* **1988**, *241*, 1176.
(46) Allara, D. L.; Wang, Z.; Pantano, C. G. *J. Non-Cryst. Solids* **1990**, *120*, 93.
(47) Neagu, R. M.; Neagu, E. R.; Kalogeras, I. M.; Vassilikou-Dova, A. *Mater. Res. Innovations* **2001**, *4*, 115.
(48) Porter, C. E.; Plum, F. D. *Macromolecules* **2000**, *33*, 7016.
(49) Stevels, J. M. *J. Non-Cryst. Solids* **1985**, *73*, 165.
(50) Fontanella, F.; Johnston, R. L.; Sigel, G. H., Jr. *J. Non-Cryst. Solids* **1979**, *31*, 401.
(51) Hunkliger, S.; Schickfus, M. V. In *Amorphous Solids Low Temperature Properties*; Phillips, W. A., Ed.; Topics in Current Physics, Vol. 24; Springer: Berlin, 1981; Chapter 6.
(52) Mahle, S. H.; McCammon, R. D. *Phys. Chem. Glasses* **1969**, *10*, 222.
(53) Barland, M.; Duval, E.; Achibat, T.; Boukenter, A. *Radiat. Eff. Defects Solids* **1995**, *137*, 191.
(54) Wallace, S.; Hench, L. L. *J. Sol−Gel Sci. Technol.* **1994**, *1*, 153.
(55) Kamiyoshi, K.; Ripoche, J. *J. Phys. Radium* **1958**, *19*, 943.
(56) Nair, N. K.; Thorp, J. M. *Trans. Faraday Soc.* **1965**, *61*, 963.
(57) Gengembre, L.; Carru, J. C.; Chapoton, A.; Vandorpe, B. *J. Chim. Phys.* **1979**, *76*, 959.
(58) Da Silva, A.; Donoso, P.; Aegerter, M. A. *J. Non-Cryst. Solids* **1992**, *145*, 168.
(59) Zhilenkov, I. V.; Nekrasova, E. G. *Russ. J. Phys. Chem.* **1980**, *54*, 1503.
(60) Yamamoto, K.; Namikara, H. *Jpn. J. Appl. Phys.* **1995**, *27*, 1845.
(61) Drotning, W. D.; Roth, E. P. *J. Mater. Sci.* **1989**, *24*, 3137.
(62) Deshpande, A. V.; Namdas, E. B. *J. Lumin.* **2000**, *91*, 25.
(63) Costela, A.; Garcia-Moreno, I.; Figuera, J. M.; Amat-Guerri, F.; Sastre, R. *Appl. Phys. Lett.* **1996**, *68*, 593.
(64) Brower, S. C.; Heyden, L. M. *J. Polym. Sci. Phys.* **1998**, *36*, 1013.
(65) Pauling, L. *The Nature of the Chemical Bond*; Cornell University Press: Ithaca, NY, 1960.
(66) Del Monte, F.; Mackenzie, J. D.; Levy, D. *Langmuir* **2000**, *16*, 7377.
(67) Mezghani, S.; Lamure, A.; Lacabanne, C. *J. Polym. Sci. Phys.* **1995**, *33*, 2413.
(68) Sauer, B. B.; Avakian, P. *Polymer* **1992**, *33*, 5128.
(69) Moura Ramos, J. J.; Mano, J. F.; Sauer, B. B. *Polymer* **1997**, *38*, 1081.
(70) Hu, L. L.; Jiang, Z. H. *Opt. Commun.* **1998**, *148*, 275.
(71) Arbeloa, F. L.; Arbeloa, T. L.; Arbeloa, I. L.; Costela, A.; GarciaMoreno, I.; Figuera, J. M.; AmatGuerri, F.; Sastre, R. *Appl. Phys. B* **1997**, *64*, 651.
(72) Muzeau, E.; Vigier, G.; Vassoille, R.; Perez, J. *Polymer* **1995**, *36*, 611.
(73) Somasundaram, G.; Ramalingam, A. *J. Photochem. Photobiol., A* **1999**, *125*, 93.
(74) Wadsworth, W. J.; Griffin, S. M.; McKinnie, I. T.; Sharpe, J. C.; Woolhouse, A. D.; Haskell, T. G.; Smith, G. J. *Appl. Opt.* **1999**, *38*, 2504.
(75) Rahn, M. D.; King, T. A. *SPIE Sol−Gel Opt. III* **1994**, *2288*, 382.
(76) Gvishi, R.; Narang, U.; Bright, F. V.; Prasad, P. N. *Chem. Mater.* **1995**, *7*, 1703.
(77) El-Shahawy, M. A.; Mansour, A. F.; Hashem, H. A. *Indian J. Pure Appl. Phys.* **1998**, *36*, 78.
(78) El-Shahawy, M. A. *Polym. Test.* **1999**, *18*, 389.